IEEE Access
Multidisciplinary | Rapid Review | Open Access Journal

Received December 27, 2020, accepted January 9, 2021, date of publication January 12, 2021, date of current version January 21, 2021.

Digital Object Identifier 10.1109/ACCESS.2021.3051200

Study on the Preparation and Test of Hydrodynamic Focusing Microfluidic Chip Fabricated by Liquid Crystal Display Mask Photo-Curing Method

JIAQING XIE[1], XIAOYU MENG[1], HAORAN PANG[1], QIAN YU[2], ZHIKANG ZHOU[1], AND FANGCHAO WANG[1]

[1]College of Mechanical and Electronic Engineering, Northwest A&F University, Yangling 712100, China
[2]Key Laboratory of Fundamental Science for Advanced Machining, Beijing Institute of Technology, Beijing 100811, China

Corresponding author: Jiaqing Xie (xiejq@nwafu.edu.cn)

This work was supported in part by the China Postdoctoral Science Foundation under Grant 2019M653761, and in part by the Provincial Innovation and Entrepreneurship Training Program of Northwest A&F University under Grant S201910712099.

ABSTRACT Microfluidic chips with the function of hydrodynamic focusing is widely used in the field of cell electroporation, droplet formation, drug screening and particle enrichment. Due to the small channel size of microfluidic chip, the existing processing methods have the defects of high fabrication cost or low dimensional consistency, the drawback is particularly prominent at small fabrication quantity. In this study, hydrodynamic focusing microfluidic chip was successfully fabricated by Liquid Crystal Display (LCD) mask photo-curing method with high efficiency and precision, the mechanism of curing parameters on the accuracy of microstructure was investigated, the hot pressing process was proposed to realize the bonding of cured photosensitive resin and glass substrate. By analyzing the focusing width of typical cross structure channel, a hydrodynamic focusing chip was designed. The effects of exposure time and single layer thickness on whole curing time was studied, the factors affecting the surface roughness were investigated, and the dimensional accuracy control method was proposed. The effect of bonding pressure on cured resin temperature was calculated and tested. The focusing width was verified by theoretical calculation and experiment. The mechanism for the inconsistency between the experimental focusing width and the theoretical focusing width was analyzed. The research proposed a solution of microfluidic design, fabrication, bonding and testing, which could provide a theoretical and methodological support for the efficient fabrication of microfluidic chips.

INDEX TERMS Hydrodynamic focusing, microfluidic chip, LCD mask photo-curing, exposure time, bonding.

NOMENCLATURE

w_0	width of the outlet channel (m)
w_i	width of the inlet channel (m)
w_s	width of the side channel (m)
w_f	focused width of the fluid (m)
h	height of channel (m)
Q_i	volumetric flow rate of the inlet channel ($\mu L \cdot min^{-1}$)
Q_{s1}	volumetric flow rate of side channel 1 ($\mu L \cdot min^{-1}$)
Q_{s2}	volumetric flow rate of side channel 2 ($\mu L \cdot min^{-1}$)
γ	velocity ratio
T	instantaneous temperature (°C)
t	time (s)
a	thermal diffusivity ($W \cdot m^{-1} \cdot °C^{-1}$)
$\dot{Q}$	heat generation rate per unit volume ($W \cdot m^{-2}$)
ρ	material density ($kg \cdot m^{-3}$)
c	specific heat capacity ($J \cdot kg^{-1} \cdot W^{-1}$)
∇	Laplacian operator
σ	the total stress
D^{el}	the fourth-order elasticity tensor
ε^{el}	the total elastic strain

The associate editor coordinating the review of this manuscript and approving it for publication was Shunfeng Cheng.

θ	interface thermal resistance ($°C^{-1}·W$)
k_1	thermal conductivity of contacting body 1 ($W·m^{-1}·°C^{-1}$)
k_2	thermal conductivity of contacting body 2 ($W·m^{-1}·°C^{-1}$)
σ_1	roughness of contacting body 1 (μm)
σ_2	roughness of contacting body 2 (μm)
E_1	elastic modulus of contacting body 1 (MPa)
E_2	elastic modulus of contacting body 2 (MPa)
v_1	Poisson's ratio of contacting body 1
v_2	Poisson's ratio of contacting body 2
C_d	curing depth (m)
D_d	single layer thickness (m)
E_0	the maximum surface exposure intensity ($cd·m^{-2}$)
E_c	exposure density ($cd·m^{-2}$)
P_L	the power of UV light (cd)
W_0	the spot radius (m)
V_s	the exposure speed ($m·min^{-1}$)

I. INTRODUCTION

Microfluidic chips with the function of hydrodynamic focusing is widely applied in the field of cell electroporation, droplet formation, drug screening and particle enrichment [1]–[6]. The dimension of microchannels and components inside the microfluidic chip ranges from several microns to hundreds of microns. Existing fabrication methods of microfluidic chips including hot embossing, microinjection molding, cast molding, laser abscission, and LIGA (Lithgraphie, Galanoformung and Abformung) method, these solutions either have the defects of high cost, low efficiency or high requirements for equipment. For example, the development cost of mold for micro injection molding or hot embossing usually ranges from US $10000 to US $100000 and the development cycle usually takes one to several months, while the LIGA technology relies on expensive equipment and complex operation process, which is especially unfriendly for the fabrication of microfluidic chips in small and medium quantities [7], [8].

Additive manufacturing technology [9], [10] has the advantages of cost effective and flexibility, which is an ideal method for microfluidic chip preparation, especially in the case of small fabrication quantity. Some miniaturized microfluidic chips have been fabricated by additive manufacturing technology, such as functional structure, microvascular networks and scaffolds. However, the additive manufacturing also has the defects of low dimensional accuracy or poor surface quality, especially in the preparation of micro scale structures [11]. Currently, the additive manufacturing method used for microfluidic chip processing mainly includes fused deposition manufacturing and ultraviolet (UV) curing methods, each method contains many branches. Dang *et al.* [12] presented a simple method to fabricate a new microfluidic-based multiplexed biosensing device by combining the FDM and the molding process. The device is an integration of normally closed microfluidic valving units which offer superior operational flexibility by using polydimethylsiloxane (PDMS) membrane and require minimized energy input. The cross-section shape and surface roughness of printed structures have not been investigated, which has a significant influence on the performance of the chip. Frederik *et al.* [13] developed two exemplary microfluidic gradient generators with a channel width and height of 800 μm and 600 μm. The designed microfluidic chip was successfully printed by a commercial benchtop stereolithography printer with a single layer thickness of 50 μm. However, the variation of surface roughness was not investigated, and the high layer thickness makes it difficult to control the channel size. Hamad *et al.* [14] demonstrate a fabrication method for fully printed microfluidic systems with sensing elements using inkjet and stereolithographic 3D-printing. Three dimensions of the microfluidic channel was printed using the polyvinylpyrrolidone-co-polymethylmethacrylate (PVP-co-PMMA) ink onto the PQA1M (Teijin Du Pont Films) substrate, after bonding, the fabricated device without any further surface modification can be used on blood test. Although the fabrication process of the chip is simplified, it is easy to cause channel blockage during the bonding process caused by the flow of photosensitive resin. Moreover, many new additive manufacturing methods for micro/nano structures have been developed, including micro stereolithography, two-photon lithography, near-field direct writing and so on [15]–[18]. The micro stereolithography and two-photon lithography method are more suitable for the mold fabrication of PDMS material chip. The near-field direct writing method can control the channel size conveniently, which have potential application value in microfluidic chip fabrication, however, the cross-section shape of the channel is difficult to control [19].

The above research proved that additive manufacturing method is feasible in the field of microfluidic machining, the UV curing method has higher fabrication accuracy than the fused deposition manufacturing method. In addition, the existing research mainly focuses on the realization of microfluidic function, but the influence of printing accuracy on the focusing width was rarely analyzed before. Therefore, it is necessary to study the fabrication methods of hydrodynamic focusing microfluidic chip with micron scale channels, develop new UV curing method with controllable cross-section size and high surface quality, as well as high fabrication efficiency. In addition, the convenience of chip bonding process is also an important factor to be considered.

In this study, a low cost and convenient preparation method of microfluidic chips with high precision was proposed. A hydrodynamic focusing microfluidic chip was designed and successfully fabricated by using a self-developed desktop LCD mask photo-curing machine based on UV curing principle, and the factors influencing the hydrodynamic focusing effect were analyzed. Firstly, the focusing width of hydrodynamic focusing microfluidic chip was verified by theoretical calculation. Secondly, the effects of exposure time and single layer thickness on whole printing time was studied, the

TABLE 1. Hydrodynamic parameters of the liquid used in the experiment.

Parameter	Value
Density ($kg{\cdot}m^{-3}$)	1000
Viscosity at 25 ºC (mpa·s)	1.005
Dynamic viscosity ($m^2{\cdot}s^{-1}$)	1.010×10^{-6}

factors affecting the surface roughness were investigated, and the dimensional accuracy control method was proposed. The effect of bonding pressure on resin temperature was investigated. Thirdly, the causation for the inconsistency between the experimental focusing width and the theoretical focusing width was analyzed. The research proposed a solution of microfluidic design, fabrication, bonding and testing, which could provide a theoretical and methodological support for the efficient fabrication of microfluidic chips.

II. EXPERIMENTS

A. THEORETICAL CALCULATION OF HYDRODYNAMIC FOCUING CHIP

The schematic illustration of symmetric hydrodynamic flow focusing of rectangular section channel is shown in Figure 1. According to the analysis of Lee *et al.* [20], the focusing width can be obtained by solving its numerical solution through the following formula,

$$\frac{w_f}{w_0} = \frac{Q_i}{\gamma(Q_i + Q_{s1} + Q_{s2})} \tag{1}$$

$$\gamma = \frac{\left\{1 - (192h/\pi^5 w_f)\sum_{n=0}^{\infty}\frac{1}{(2n+1)^5}\frac{sinh[(2n+1)\pi w_f/2h]}{cosh[(2n+1)\pi w_0/2h]}\right\}}{\left\{1 - (192h/\pi^5 w_0)\sum_{n=0}^{\infty}\frac{tanh[(2n+1)\pi w_0/2h]}{(2n+1)^5}\right\}} \tag{2}$$

where γ is the velocity ratio, w_0 is the width of the outlet channel, w_i is the width of the inlet channel, w_s is the width of the side channel, w_f is the focused width of the fluid, h is the height of channel, Q_i is the volumetric flow rate of the inlet channel, Q_{s1} and Q_{s2} is volumetric flow rate of side channel 1 and 2, respectively.

B. MATERIALS AND SAMPLE PREPARATION

The liquid used in the hydrodynamic focusing test is purified water mixed with different colors of ink, the hydrodynamic parameters are shown in Table 1.

The physical and chemical parameters of photosensitive resin (CREALITY, Co., Ltd, China) parameters used in the experiment is shown in Table 2. The cured resin has good light transmittance and high mechanical strength, which can guarantee the chip's optical properties and mechanical requirements [21].

The optical glass wafer (D-ZK3, CDGM GLASS Co., Ltd, Chengdu, China) [21], with a 76.2 mm length, 25.4 mm width and 0.8 mm thickness was used in the experiment. The material is dense barium crown optical glass with a transition temperature of 511 °C, which can ensure the stability of

TABLE 2. Photosensitive resin parameters applied in experiments.

Photosensitive resin parameters	Range
Shrinkage rate (%)	3.72-4.24
Solidification wavelength (nm)	355-410
Thermal deformation temperature(ºC)	80
Viscosity at 25 ºC (mpa·s)	150-200

TABLE 3. Thermo-mechanical properties of glass, polymer and mold [23].

Materials	Glass	Polymer	Stainless steel
Density ($Kg{\cdot}m^{-3}$)	2990	1048	7800
Elastic modulus (GPa)	83.6	2.48(20 ºC) 2.25(70 ºC)	210
Thermal conductivity ($W{\cdot}m^{-1}{\cdot}ºC^{-1}$)	1.028	0.15	44
Specific heat ($J{\cdot}kg^{-1}{\cdot}ºC^{-1}$)	910	72	502
Linear expansion coefficient ($ºC^{-1}$)	7.2×10^{-6}	6.7×10^{-6}	12.2×10^{-6}
Poisson ratio	0.28	0.31(20 ºC) 0.40(70 ºC)	0.3

physical and chemical properties during bonding process. The thermo-mechanical properties of the cured polymer were tested systematically, while the thermo-mechanical properties of glass and the stainless steel have been obtained in our previous research, as shown in Table 3 [22].

C. SIMULATION OF BONDING PROCESS

In order to determine the mechanism of bonding parameters on the bonding effect of microfluidic chips, a temperature-displacement coupling simulation of bonding process was carried out. The governing differential equation of unsteady heat conduction can be expressed as [23]

$$\frac{\partial T}{\partial t} = a\nabla^2 T + \frac{\dot{Q}}{\rho c} \tag{3}$$

where T denotes the instantaneous temperature, t gives the time, a is thermal diffusivity, $\dot{Q}$ gives the heat generation rate per unit volume, ρ is the material density, c is the specific heat capacity, ∇ is Laplacian operator.

The linear elastic constitutive model considering temperature variation was applied to the thermal mechanical coupling simulation. The total stress is defined from the total elastic strain as,

$$\sigma = D^{el}\varepsilon^{el} \tag{4}$$

where σ is the total stress, D^{el} is the fourth-order elasticity tensor, ε^{el} is the total elastic strain.

An interface thermal resistance model [22] was adopted to calculate the effect of temperature and pressure on interface thermal resistance between glass, cured resin and stainless steel.

$$\theta = \frac{2.55(k_1+k_2)(E_1E_2)^{\frac{1}{3}}(\sigma_1^2+\sigma_2^2)^{\frac{5}{6}}}{P^{\frac{1}{3}}k_1k_2\left[\left(1-v_1^2\right)E_2+\left(1-v_2^2\right)E_1\right]^{\frac{1}{3}}} \tag{5}$$

where θ is the interface thermal resistance, k_1, k_2 refer to the thermal conductivity of the contacting bodies, σ_1, σ_2 are the contact roughness, E_1, E_2 are the elastic modulus, and v_1, v_2 are the Poisson's ratio.

D. CHARACTERIZATION AND INSTRUMENTS

A self-developed LCD mask photo-curing machine was adopted for light curing process, the machine includes platform, Z axis, material trough and LCD panel. The cured parts attach to the platform during the curing process, the Z axis controls the platform movement, and the photosensitive resin is laid out on the material trough. Figure 2 is the schematic diagram of LCD mask photo-curing machine, the incident position of light source can be controlled by LCD panel, the light source is homogenized by Fresnel lens. The minimum resolution of the LCD panel is 5 μm, the Z axis resolution is 1.5 μm. The minimum single layer printing thickness can be reduced to 10 μm, and the maximum curing speed is 20 mm·h^{-1}. Minimal single layer printing thickness can reduce the shape error of the cured parts and improve the surface quality, which is beneficial to the accurate preparation of microchannel.

The UV light was adopted as the light source, the absorption of UV light by photosensitive resin accords with Beer-Lambert theorem, The energy of UV light decreases exponentially with the depth of irradiation. When the energy density is greater than the critical exposure density E_c of the photosensitive resin, the photosensitive resin will solidify. The curing depth C_d can be expressed as,

$$C_d = D_d ln \frac{E_0}{E_c} \tag{6}$$

The intensity of UV light source accords with Gaussian distribution theorem, the maximum surface exposure intensity E_o is

$$E_o = \sqrt{\frac{2}{\pi}} \frac{P_L}{W_0 V_s} \tag{7}$$

where D_d is the single layer thickness, P_L is the power of UV light, W_0 is the spot radius, V_s is the exposure speed [24], [25].

A self-developed hot press machine was applied for bonding process, the machine includes upper heating plate, lower heating plate and manual control area. The maximum pressure is 40 MPa, the maximum heating temperature is 300 °C, and the temperature control error is less than 1 °C. The bonding process parameters are controlled by a computer connected to the machine. The temperature-displacement coupling simulation of bonding process was carried out by using the commercially available FEM code ABAQUS. The schematic diagram of temperature-displacement coupling simulation model is shown in Figure 3. The bonding pressure was controlled by the upper heating plate, while the lower heating plate remained fixed. The temperature of the contact surface between glass and resin was observed.

A test method was developed to evaluate the numerical results by installing a micro thermocouple probe between the interfaces of bonded parts. The micro thermocouple probe is cylindrical with a diameter of 0.3 mm and length of 2 mm, respectively. The detection accuracy of micro thermocouple is 0.1 °C. The temperature rise curves with different loading pressure were collected and stored by digital temperature recorder (Dongtai iredi Technology Co., Ltd, China), which could be compared with the simulation results. In order to ensure that the bonding pressure was not affected by the micro thermocouple, the cured chip was reserved with a micro hole to place the sensor. The diagram of the test system is shown in Figure 4.

The test system of microfluidic chip is shown in Figure 5, during the hydrodynamic focusing test, the liquid is pushed into the microfluidic chip channel through the syringe driven by the micro injection pump (XFP02-B, Suzhou iFLYTEK Scientific Instrument Co., Ltd, China), the liquid flow rate is controlled by micro injection pump. The video of the fluid focusing process is obtained by the combination of optical module and high-speed CCD (815UM, Weihong image Co., Ltd, China), and transmitted to the laptop. The field light intensity is controlled by an LED light. The surface roughness of cured part was observed by the laser microscope (VHX-1000, KEYENCE Co., Ltd, Japan) with display resolution of height 0.005 μm and width 0.01 μm. The numerical solution of the focusing width was obtained by MATLAB 2018 (Mathworks Inc, America) software.

III. RESULTS AND DISCUSSION

A. DESIGN OF HYDRODYNAMIC FOCUING CHIP

According to the equation 1 and 2, the focusing width is mainly related to the velocity and width of the channel, and the channel depth mainly affects the flux of the focused liquid. A hydrodynamic focusing microfluidic chip with three dimensional dimensions of 55 mm length, 25.4 mm width and 3 mm thickness was designed, the focusing chip includes three inlets and outlets respectively. The channel width of the chip is 300 μm and the height is 350 μm, as shown in Figure 6.

B. INFLUENCE OF UV CURING PARAMETERS ON MICROFLUIDIC CHIP CHANNEL ACCURACY

Before preparing the designed microfluidic chip, it is necessary to investigate the influence of curing parameters on printing time, surface quality and shape accuracy. The effects of exposure time and single layer thickness on whole printing time is shown in Figure 7. The experimental results demonstrate that increasing the single layer thickness can reduce the whole printing time significantly, and the exposure time does not play a major role in the whole printing time.

The relationship between UV exposure time and surface roughness of cured parts at different single layer thickness is shown in Figure 8. When the thickness of single layer printing is less than 20 μm, the final surface roughness first decreases and then slightly increases, the experiment proved that small single layer thickness cannot guarantee good surface quality. If the UV exposure time is less than 2 s, the photosensitive

resin cannot be fully cured, resulting in high surface roughness. With the increase of exposure time, the surface roughness decreases sharply. When the exposure time is 6 s, the surface roughness decreases to the minimum of 0.171 μm. Once the exposure time is more than 6 s, the whole microstructure cannot be fabricated. After considering the two factors of printing efficiency and printing accuracy, the exposure time of 6 s and the printing thickness of 50 μm were adopted to fabricate the designed hydrodynamic focusing microfluidic chip.

Based on the analysis of equation 6 and 7, the attenuation of light source energy density has a significant effect on the shape of cured parts. In addition, the volume shrinkage of the photosensitive resin during the curing process and the movement accuracy of the equipment will affect the dimensional accuracy of the cured parts. Therefore, there will have a certain deviation between the designed size and the actual preparation size during the LCD mask photo-curing process. In order to accurately prepare the rectangular microgroove with the target size, it is necessary to analyze the corresponding relationship between the designed size and the actual microchannel size. In the experiment, the exposure time was 6 s, each experiment was conducted for three times, the size error of cured rectangular microchannel is less than 0.02 μm, and the tested results are fitted in a straight line, as shown in Figure 9. The straight line fitting formulas of width and height are $y = 0.915x - 38.467$ and $y = 0.871x - 21.867$, while the R square is 0.964 and 0.989, respectively. The results show that the repeatability error of width and height direction are very small when the curing parameters keep consistent. The minimum channel size that can be machined by LCD mask photo-curing method can reach 100 μm, and the surface quality are significantly better than correlational research reported recent years [26]–[28].

According to the above research, a rectangular cross-section microfluidic chip with a width of 300 μm and a depth of 350 μm was prepared. The micrograph of the fabricated microfluidic chip is shown in Figure 10(a), the size of the channel is uniform, but there are smaller arcs at the cross of the channel, the reason for this phenomenon is that the spot radius is fixed during the curing process, it is unable to reduce the spot radius according to the structure shape, resulting in incomplete curing at the corner. Except the cross position, the cured microchannel has high size consistency, the three-dimensional structure of the channel is shown in Figure 10(b). The cross-section shape of the microchannel is shown in Figure 10(c), the results indicated that after curing parameter adjustment, the LCD mask photo-curing machine can realize high precision fabrication of microchannel.

C. EFFECT OF BONDING PRESSURE ON HEATING TEMPERATURE OF PHOTOSENSITIVE RESIN

The surface roughness of stainless steel, cured resin and glass is 1.6 μm, 0.171 μm and 0.01 μm, respectively. Based on the equation 5, the effects of pressure on interface thermal resistance is obtained, as shown in Figure 11. The curves indicate that there is a negative correlation between contact pressure and thermal resistance coefficient. In addition, low surface roughness is more conducive to the reduction of thermal resistance coefficient

The comparison of the temperature rises of resin at different bonding pressure is shown in Figure 12. During the experiment, the temperature of the upper and lower heating plates of the hot press machine was kept at 80 °C, and the test chip was heated as soon as it was put in. Therefore, only the temperature rise date after the microfluidic chip was stably applied pressure was extracted. The simulation results and tested results both confirmed that the resin temperature rises rapidly with the increase of bonding pressure. The increased bonding pressure reduces the interface thermal resistance between the heating platform, resin and glass. However, the increase of pressure has no obvious effect on the total heating time. Therefore, it is not necessary to blindly increase the pressing pressure during bonding process, which is beneficial to reduce the channel deformation of microfluidic chip. It should be noted that the rising speed of temperature in the experiment is slower than that in the simulation, and it is necessary to continue to optimize the thermal resistance model in the follow-up research. Besides, the effect of bonding pressure on bonding strength of glass and cured resin needs to be further investigated.

Based on the simulation and test result, the prepared microfluidic chip was fixed on the glass substrate by hot bonding process. The bonding temperature is 80 °C, the bonding pressure is 0.2 MPa, and the holding time is 1 hour. The chip inlet and outlet were connected by ruhr connector, and the connectors were glued together. The assembled microfluidic chip is shown in Figure 13. By water injection test, the glass substrate and the cured resin microfluidic chip were well bonded without leakage.

The core equipment of the whole hydrodynamic focusing chip preparation is a simple desktop device. It can be completed by printing, cleaning and bonding process, the overall process shows the superiority of high efficiency and cost-effectively [29]–[31].

D. HYDRODYNAMIC FOCUSING EXPERIMENT

The experimental images of the symmetric hydrodynamic focusing effect in microchannel with different flow rate ratios are shown in Figure 14. Different from the theoretical model, there is a certain fillet in the cross position of the microfluidic chip fabricated by LCD mask photo-curing method, the fillets may affect the focus width.

The comparison of focusing width of theory and experiment result under different flow rate ratios is shown in Figure 15. The variation trend of focusing width is consistent with the theoretical calculation, but there is a certain gap between the experimental results and the theoretical results of hydrodynamic focusing. When the flow rate ratio is less than 1, the experimental focusing width is larger than the theoretical calculation width, once the flow rate ratio is greater

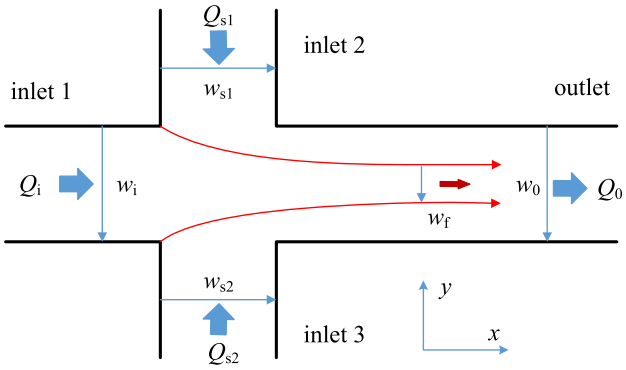

FIGURE 1. Schematic illustration of symmetric hydrodynamic flow focusing.

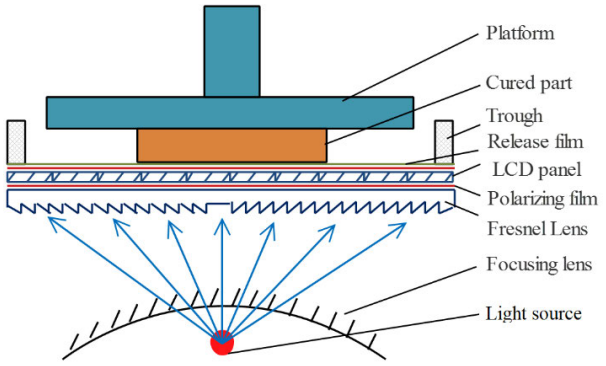

FIGURE 2. Schematic diagram of self-developed LCD mask photo-curing machine.

than 1, the experimental focusing width is smaller than the theoretical calculation.

In order to analyze the reasons for the inconsistency between the experimental focusing width and the theoretical focusing width, the influence of microchannel width on focusing width at different flow rate ratios are investigated by simultaneous equation 1 and 2, as shown in Figure 16. During the calculation, the flow rate and microchannel depth of inlet 1 remain constant. It can be seen from the results that there is a linear relationship between the channel width and the focus width. When the flow rate ratio is less than 1, the focus starting position is far away from the inlet 1. Because of the existence of fillet at the junction, the actual channel width is larger than the designed width, resulting in the increase of focus width. Otherwise, the actual focus width is reduced.

Due to the limitation of LCD screen resolution and equipment motion accuracy, it is difficult to eliminate the fillet at the intersection of micro channels. In the follow-up study, the corner radius of microchannel will be reduced by increasing the resolution of LCD screen to 4K and improving the accuracy of the motion system. In addition, developing the resin with lower shrinkage is also a major means to improve printing accuracy, which needs further efforts.

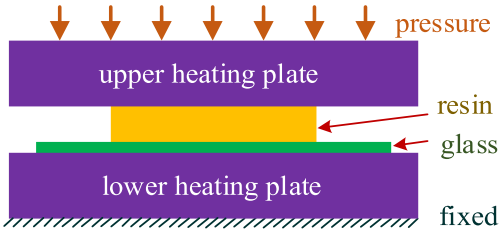

FIGURE 3. Schematic diagram of temperature-displacement coupling simulation model.

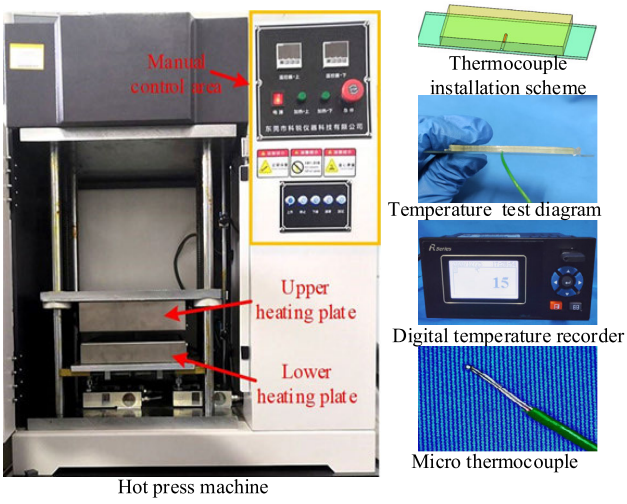

FIGURE 4. Diagram of temperature curve acquisition method.

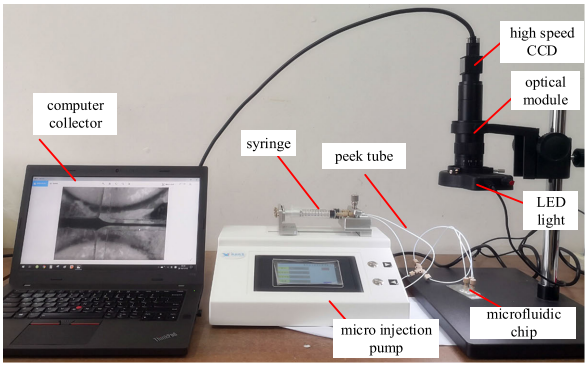

FIGURE 5. The test system of hydrodynamic focusing microfluidic chip.

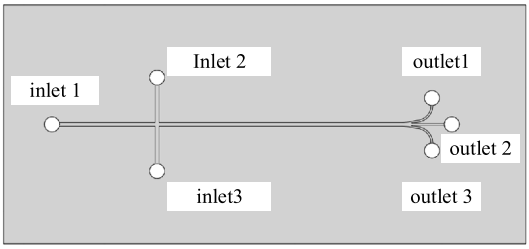

FIGURE 6. Schematic diagram of designed hydrodynamic focusing microfluidic chip.

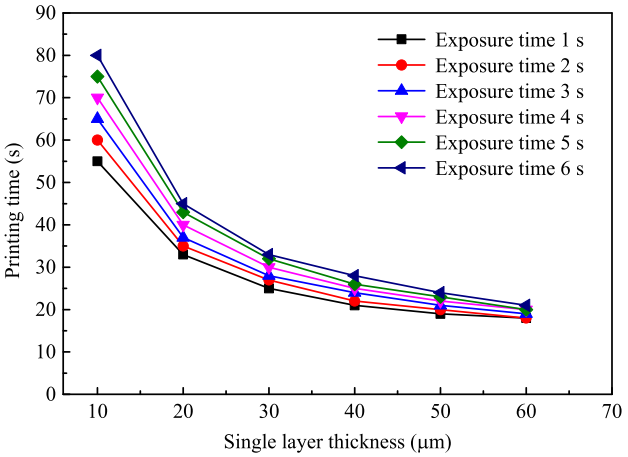

FIGURE 7. The effects of exposure time and single layer thickness on whole printing time.

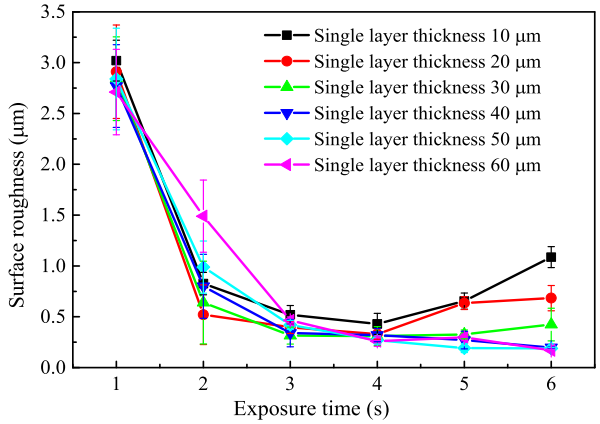

FIGURE 8. Relationship between UV exposure time and surface roughness.

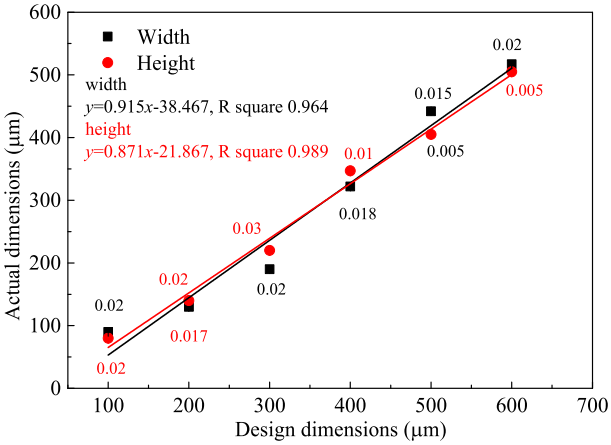

FIGURE 9. Relationship between design dimensions and actual dimensions.

IV. CONCLUSION

This research provided a low-cost, fast and high-precision microfluidic chip preparation method for small and medium-batches. The hydrodynamic focusing microfluidic chip with a

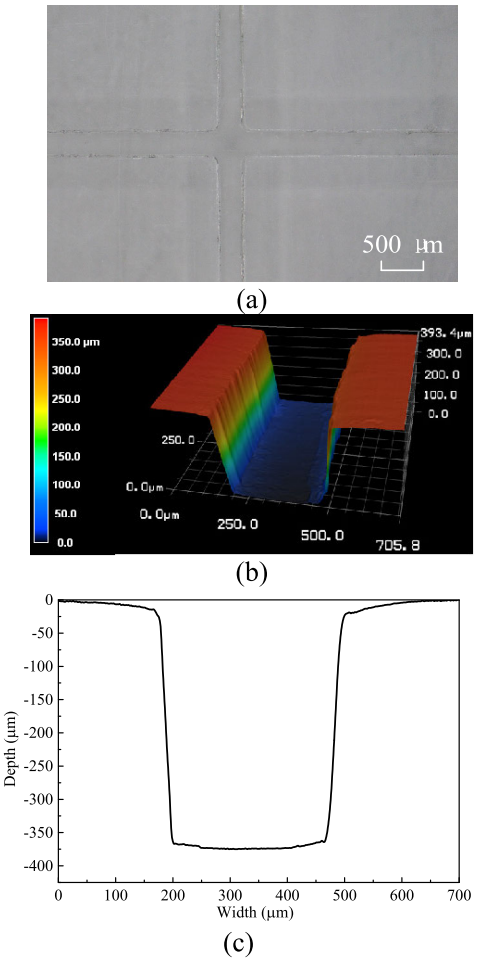

FIGURE 10. The fabricated microfluidic chip: (a) micrograph photograph, (b) three-dimensional structure, and (c) the cross-section shape.

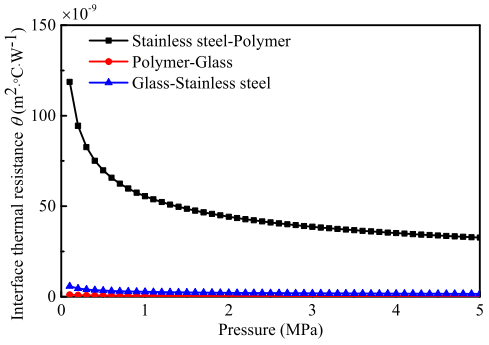

FIGURE 11. Effects of pressure on interface thermal resistance.

width of 300 μm and depth of 350 μm was designed and fabricated by using a self-developed desktop LCD mask photo-curing machine, then bonded with hot pressing method. The mechanism of curing parameters on the accuracy of microstructure was investigated, the surface roughness of the cured parts could be minimized to 0.171 μm with an exposure time of 6 s. The cured resin was well bonded on glass substrate at a bonding temperature of 80 °C, and bonding

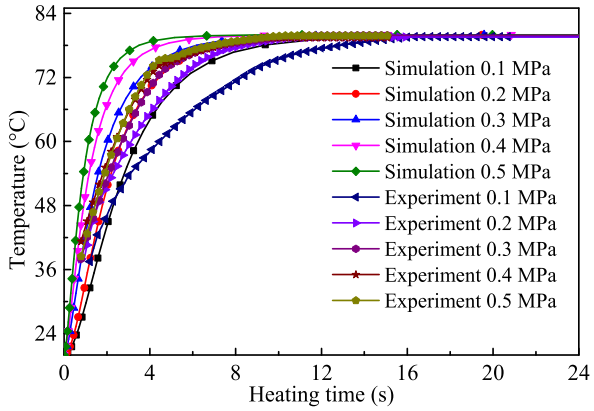

FIGURE 12. Comparison of the temperature rise of resin at different bonding pressure.

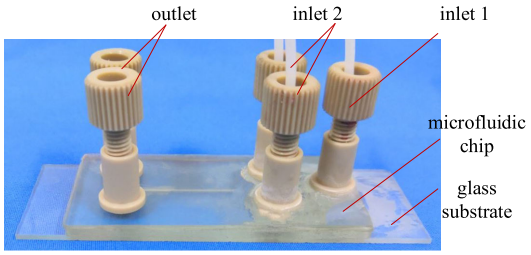

FIGURE 13. Fabricated microfluidic chip after bonding.

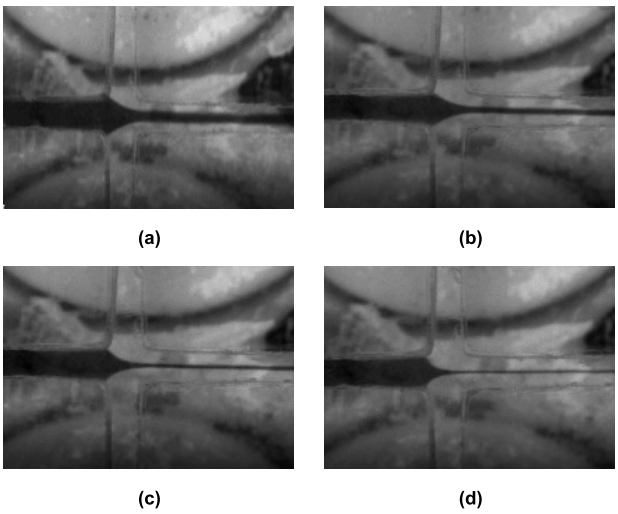

FIGURE 14. Experimental images of the symmetric hydrodynamic focusing effect in microchannels with different flow rate ratios (Q_s/Q_i): (a) $Q_s/Q_i = 0.5$, (b) $Q_s/Q_i = 1.0$, (c) $Q_s/Q_i = 1.5$, (d) $Q_s/Q_i = 2.0$.

pressure of 0.2 MPa for 1 hour. The inconsistency between the experimental focusing width and the theoretical focusing width was mainly caused by the fillet at the junction of the cured channel. The fabrication methods mentioned above should facilitate the prototyping of devices for microfluidics, and conducived to the rapid development of the microfluidics. In addition, the following research should further improve the preparation accuracy of complex structure shape, such

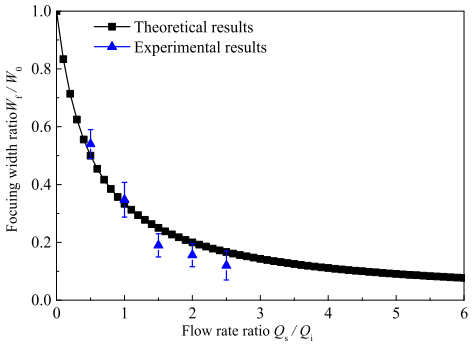

FIGURE 15. Comparison of focusing width of theoretical calculation and experiment result under different flow rate ratios.

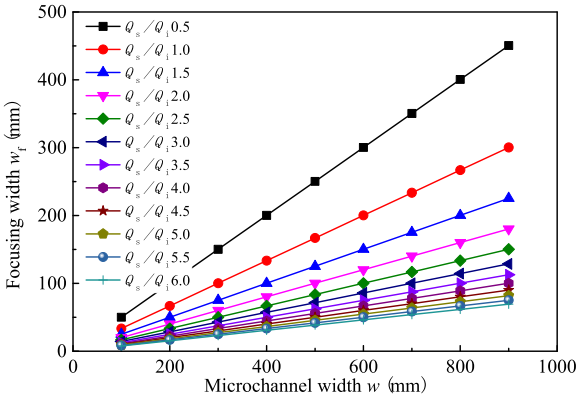

FIGURE 16. The influence of microchannel width on focusing width at different flow rate ratios.

as increasing LCD screen resolution, reducing the volume shrinkage of photosensitive resin and improving the motion accuracy of LCD mask photo-curing machine.

REFERENCES

[1] B. Zhu, Y. Cai, Z. Wu, F. Niu, and H. Yang, "Dielectrophoretic microfluidic chip integrated with liquid metal electrode for red blood cell stretching manipulation," *IEEE Access*, vol. 7, pp. 152224–152232, 2019.
[2] Y. Fan, D. Dong, Q. Li, H. Si, H. Pei, L. Li, and B. Tang, "Fluorescent analysis of bioactive molecules in single cells based on microfluidic chips," *Lab a Chip*, vol. 18, no. 8, pp. 1151–1173, 2018.
[3] Z. Jiao, L. Zhao, C. Tang, H. Shi, F. Wang, and B. Hu, "Droplet-based PCR in a 3D-printed microfluidic chip for miRNA-21 detection," *Anal. Methods*, vol. 11, no. 26, pp. 3286–3293, 2019.
[4] Y. Chiu, S. Cho, Z. Mei, V. Lien, T. Wu, and Y. Lo, "Universally applicable three-dimensional hydrodynamic microfluidic flow focusing," *Lab a chip*, vol. 13, no. 9, pp. 1803–1809, 2013.
[5] P. Cui and S. Wang, "Application of microfluidic chip technology in pharmaceutical analysis: A review," *J. Pharmaceutical Anal.*, vol. 9, no. 4, pp. 238–247, Aug. 2019.
[6] U. Masud, F. Jeribi, A. Zeeshan, A. Tahir, and M. Ali, "Highly sensitive microsensor based on absorption spectroscopy design considerations for optical receiver," *IEEE Access*, vol. 8, pp. 100212–100225, 2020.
[7] S. A. Wirdatmadja, D. Moltchanov, S. Balasubramaniam, and Y. Koucheryavy, "Microfluidic system protocols for integrated on-chip communications and cooling," *IEEE Access*, vol. 5, pp. 2417–2429, 2017.
[8] K. Vishnubhatla, R. Osellame, G. Lanzani, R. Ramponi, and T. Virgili, "Organic random laser in an optofluidic chip fabricated by femtosecond laser," *Proc. SPIE*, vol. 7585, Feb. 2010, Art. no. 75850E.
[9] H. Becker, B. Gray, D. Helmer, B. Rapp, and F. Kotz, "Additive manufacturing of microfluidic glass chips," *Proc. SPIE*, vol. 10491, Feb. 2018, Art. no. 104910A.

[10] Q. Zhu, M. Hamilton, B. Vasquez, and M. He, "3D-printing enabled micro-assembly of a microfluidic electroporation system for 3D tissue engineering," *Lab a Chip*, vol. 19, no. 14, pp. 2362–2372, 2019.
[11] P. Van, J. Gorecki, F. Numkam, V. Apostolopoulos, and F. Poletti, "3D-printed polymer antiresonant waveguides for short-reach terahertz applications," *Appl. Opt.*, vol. 57, no. 14, pp. 3953–3958, 2018.
[12] B. V. Dang, A. Hassanzadeh-Barforoushi, M. S. Syed, D. Yang, S.-J. Kim, R. A. Taylor, G.-J. Liu, G. Liu, and T. Barber, "Microfluidic actuation via 3D-printed molds toward multiplex biosensing of cell apoptosis," *ACS Sensors*, vol. 4, no. 8, pp. 2181–2189, Aug. 2019.
[13] K. Frederik, R. Patrick, H. Dorothea, and R. Bastian, "Highly fluorinated methacrylates for optical 3D printing of microfluidic devices," *Micromachines*, vol. 9, no. 3, pp. 115–125, 2018.
[14] E. M. Hamad, S. E. R. Bilatto, N. Y. Adly, D. S. Correa, B. Wolfrum, M. J. Schöning, A. Offenhäusser, and A. Yakushenko, "Inkjet printing of UV-curable adhesive and dielectric inks for microfluidic devices," *Lab a Chip*, vol. 16, no. 1, pp. 70–74, 2016.
[15] D. Han, C. Yang, N. X. Fang, and H. Lee, "Rapid multi-material 3D printing with projection micro-stereolithography using dynamic fluidic control," *Additive Manuf.*, vol. 27, pp. 606–615, May 2019.
[16] N. Duangrit, B. Hong, A. D. Burnett, P. Akkaraekthalin, I. D. Robertson, and N. Somjit, "Terahertz dielectric property characterization of photopolymers for additive manufacturing," *IEEE Access*, vol. 7, pp. 12339–12347, 2019.
[17] P. Li, T. Wu, L. Zhang, J. Chen, X. Feng, F. Huang, and C. Zuo, "Effects of the electrohydrodynamic near-field direct-writing process parameters on micro patterns," *Micronanoelectron. Technol.*, vol. 56, pp. 65–70, Feb. 2019.
[18] J. M. Monkevich and G. P. Le Sage, "Design and fabrication of a custom-dielectric fresnel multi-zone plate lens antenna using additive manufacturing techniques," *IEEE Access*, vol. 7, pp. 61452–61460, 2019.
[19] F.-L. He, D.-W. Li, J. He, Y.-Y. Liu, F. Ahmad, Y.-L. Liu, X. Deng, Y.-J. Ye, and D.-C. Yin, "A novel layer-structured scaffold with large pore sizes suitable for 3D cell culture prepared by near-field electrospinning," *Mater. Sci. Eng., C*, vol. 86, pp. 18–27, May 2018.
[20] G.-B. Lee, C.-C. Chang, S.-B. Huang, and R.-J. Yang, "The hydrodynamic focusing effect inside rectangular microchannels," *J. Micromech. Microeng.*, vol. 16, no. 5, pp. 1024–1032, May 2006.
[21] T. Wang, J. Chen, T. Zhou, and L. Song, "Fabricating microstructures on glass for microfluidic chips by glass molding process," *Micromachines*, vol. 9, no. 6, pp. 269–272, 2018.
[22] J. Xie, T. Zhou, B. Ruan, Y. Du, and X. Wang, "Effects of interface thermal resistance on surface morphology evolution in precision glass molding for microlens array," *Appl. Opt.*, vol. 56, no. 23, pp. 6622–6630, 2017.
[23] S. Zhou and J. R. Solana, "Thermodynamic properties of fluids with Lennard–Jones–Gauss potential from computer simulation and the coupling parameter series expansion," *Mol. Phys.*, vol. 116, no. 3, pp. 491–506, 2018.
[24] S. Li and Z. Wang, "Generation of optical vortex based on computer-generated holographic gratings by photolithography," *Appl. hys. Lett.*, vol. 103, no. 14, pp. 141110–141113, 2013.
[25] Z. Mei, Y. Mao, and Y. Wang, "Electromagnetic multi-Gaussian Schell-model vortex light sources and their radiation field properties," *Opt. Exp.*, vol. 26, no. 17, pp. 21992–22000, 2018.
[26] Y. Li, S. Lai, N. Liu, G. Zhang, L. Liu, and G. Lee, "Fabrication of high-aspect-ratio 3D Hydrogel microstructures using optically induced electrokinetics," *Micromachines*, vol. 7, no. 4, pp. 65–71, 2016.
[27] P. Daniela, L. Piero, F. Daniel, and P. Gianluca, "Extrusion-based 3D printing of microfluidic devices for chemical and biomedical applications: A topical review," *Micromachines*, vol. 9, no. 8, pp. 374–400, 2018.
[28] M. A. Raoufi, S. Razavi Bazaz, H. Niazmand, O. Rouhi, M. Asadnia, A. Razmjou, and M. Ebrahimi Warkiani, "Fabrication of unconventional inertial microfluidic channels using wax 3D printing," *Soft Matter*, vol. 16, no. 10, pp. 2448–2459, 2020.
[29] X. Jiang, D. F. Wang, and Z. Yin, "Manufacture of microfluidic chips using a gap-control method based on traditional 3D printing technique," *Microsyst. Technol.*, vol. 25, no. 3, pp. 1043–1050, Mar. 2019.
[30] A. Enders, I. Siller, K. Urmann, M. Hoffmann, and J. Bahnemann, "3D printed microfluidic mixers—A comparative study on mixing unit performances," *Small*, vol. 15, no. 2, 2019, Art. no. e1804326.
[31] S. Waheed, J. M. Cabot, N. P. Macdonald, T. Lewis, R. M. Guijt, B. Paull, and M. C. Breadmore, "3D printed microfluidic devices: Enablers and barriers," *Lab a Chip*, vol. 16, no. 11, pp. 1993–2013, 2016.

JIAQING XIE received the Ph.D. degree from the Beijing Institute of Technology, in 2018. He was a Postdoctoral Training with Northwest A&F University from 2018 to 2020. Since 2018, he has been an Assistant Professor with the College of Mechanical and Electronic Engineering, Northwest A&F University. He has authored or coauthored more than 30 articles and conference proceedings, and ten China patents. He is currently a member of Plastic Engineering Society of China Society of mechanical engineering, and a Senior Member of China Society of Micron and Nanotechnology. In 2015, he won the Excellent Paper Award of National Plastic Engineering Youth Academic Conference, the best Poster Award of UPM International Conference in 2017, the Third Prize of Excellent Paper Award of Shaanxi Young Scientists Conference in 2019, and the Excellent Paper Award of China Japan Ultra-Precision Machining Conference in 2019.

XIAOYU MENG was born in Weinan, Shaanxi. He is currently pursuing the degree with the Department of Vehicle Engineering, College of Mechanical and Electrical Engineering, Northwest A&F University. He is also working as a Laboratory Assistant with the Vehicle Engineering Laboratory, College of Mechanical and Electrical Engineering, Northwest A&F University. During his study, he presided over or participated in a number of innovative projects, mainly focusing on structural optimization design, cell enrichment, inertial microfluidic chip, and other fields. He wrote or co-wrote many articles, published several patents, and participated in many competitions and won awards. In this project, he is mainly responsible for structural optimization design. At present, he is committed to the development and preparation of inertial microfluidic chips with cell enrichment function.

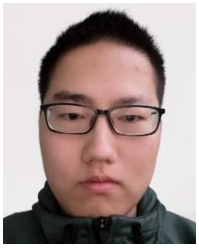

HAORAN PANG was born in Heze, Shandong. He is currently pursuing the degree with the Department of Agricultural Engineering, College of Mechanical and Electrical Engineering, Northwest A&F University. During the period of school, he mainly studied microfluidic chip, additive manufacturing, photoelectric detection, and so on. He is also working as a Laboratory Assistant with the College of Mechanical and Electrical Engineering, Northwest A&F University. The work in this article was done when he studied additive manufacturing. At present, he is committed to the development of portable rapid detection instrument for pesticide residues based on microfluidic chip.

QIAN YU received the bachelor's degree from the Beijing Institute of Technology, in 2015, where he is currently pursuing the Ph.D. degree. He has authored or coauthored ten articles and conference proceedings, and three authorized Chinese invention patents so far. He received the financial support from the China Association for Science and Technology (CAST) and the China Scholarship Council (CSC) for the Joint Ph.D. program in Tohoku University and Keio University in Japan from 2018 to 2019. In 2019, he won the Excellent Paper Award of China-Japan International Conference on Ultra-Precision Machining Process.

ZHIKANG ZHOU was born in Dongying, Shandong. He is currently pursuing the degree with the Department of Agricultural Engineering, College of Mechanical and Electrical Engineering, Northwest A&F University. He is also working as a Laboratory Assistant with the College of Mechanical and Electrical Engineering, Northwest A&F University. At present, he is committed to direct writing fabrication and testing of microfluidic chips. He is recommended to the Beijing Institute of Technology for postgraduate study. During the study period, the research interests include microfluidic chip, additive manufacturing, micro nano manufacturing, and so on.

FANGCHAO WANG received the bachelor's degree in 2010. Since 2010, he has been an Assistant Experimentalist with the College of Mechanical and Electronic Engineering, Northwest A&F University. He is mainly involved in the application and teaching of modern manufacturing technology. He has authored or coauthored more than ten articles and participated in the publication of a monograph on advanced manufacturing.